TISSUE ENGINEERING: Part A
Volume 15, Number 6, 2009

DOI: 10.1089/ten.tea.2008.0314

Prevascularization of a Fibrin-Based Tissue Construct Accelerates the Formation of Functional Anastomosis with Host Vasculature

Xiaofang Chen, M.S.,[1] Anna S. Aledia, B.S.,[1] Cyrus M. Ghajar, Ph.D.,[1] Craig K. Griffith, Ph.D.,[1] Andrew J. Putnam, Ph.D.,[1,2] Christopher C.W. Hughes, Ph.D.,[1,3] and Steven C. George, M.D., Ph.D.[1,2]

One critical obstacle facing tissue engineering is the formation of functional vascular networks that can support tissue survival *in vivo*. We hypothesized that prevascularizing a tissue construct with networks of well-formed capillaries would accelerate functional anastomosis with the host upon implantation. Fibrin-based tissues were prevascularized with capillary networks by coculturing human umbilical vein endothelial cells (HUVECs) and fibroblasts in fibrin gels for 1 week. The prevascularized tissue and nonprevascularized controls were implanted subcutaneously onto the dorsal surface of immune-deficient mice and retrieved at days 3, 5, 7 and 14. HUVEC-lined vessels containing red blood cells were evident in the prevascularized tissue by day 5, significantly earlier than nonprevascularized tissues (14 days). Analysis of the HUVEC-lined vessels demonstrated that the number and area of perfused lumens in the prevascularized tissue were significantly larger compared to controls. In addition, collagen deposition and a larger number of proliferating cells were evident in the prevascularized tissue at day 14. Our results demonstrate that prevascularizing a fibrin-based tissue with well-formed capillaries accelerates anastomosis with the host vasculature, and promotes cellular activity consistent with tissue remodeling. Our prevascularization strategy may be useful to design large three-dimensional engineered tissues.

Introduction

Tissue engineering holds enormous potential to replace or restore the function of damaged or diseased tissues.[1] However, the most successful applications have been limited to thin avascular tissues such as skin and cartilage[2,3] in which delivery of nutrients and oxygen relies on diffusion. To overcome the diffusion limit, a functional vascular network must be created to deliver blood to the inner part of the tissue quickly upon implantation.

Several approaches have been employed to vascularize engineered tissue and thus overcome diffusion limits in thick tissue. For example, controlled release of proangiogenic factors from an implant can stimulate the in growth of host vessels.[4,5] This method does not depend on an autologous cell source, but the slow growth of new vessels may compromise tissue viability.[6] Alternatively, one can seed vascular endothelial cells into the implanted tissue as a means of accelerating vessel formation.[7–11] This method relies on vasculogenesis *in situ*, and the time it takes for this process to occur may, again, compromise the implanted tissue.

An alternate method is to prevascularize the tissue with well-formed vessel networks before implantation. It has recently been demonstrated that seeding endothelial cells into a tissue construct before implantation may improve blood perfusion and tissue survival.[12,13] Although several reports describe the creation of three-dimensional capillary networks *in vitro*,[14–16] the use of this method to enhance perfusion to an implanted tissue has been limited to a skin graft.[17] Herein, we report the optimal formation of three-dimensional well-formed capillary networks with lumens in a fibrin gel, and the performance of the prevascularized tissue after subcutaneous implantation in immune-deficient mice. Our results demonstrate that the *in vitro*–formed capillaries are functional *in vivo*, and more importantly, the prevascularized tissue anastomoses with the host vasculature (4–5 days) significantly faster than nonprevascularized tissues (8–14 days). Further, tissue remodeling and cellular activity are also enhanced in the prevascularized tissue after implantation. Our tissue model provides a platform to study the *in vitro* morphology and *in vivo* function of engineered capillary networks, and may be useful to overcome the diffusion

Departments of [1]Biomedical Engineering, [2]Chemical Engineering and Materials Science, [3]Molecular Biology and Biochemistry, University of California Irvine, Irvine, California.

limit and lead to the successful design of large, three-dimensional, engineered tissues.

Materials and Methods

Cell culture

Normal human lung fibroblasts (NHLFs; American Type Culture Collection, Manassas, VA) were cultured in fibroblast growth medium with 2% fetal bovine serum (FBS) (FGM-2; Lonza, Walkersvill, MD). Human umbilical vein endothelial cells (HUVECs) were isolated from human umbilical cords as previously described[18] and grown in endothelial growth medium with 2% FBS (EGM-2; Lonza). Cells were maintained at 37°C in 100% humidified air containing 5% CO_2, and the medium was changed every other day. All the experiments utilized passage 4–8 fibroblasts and passage 3 HUVECs.

Preparation of the tissue constructs

To make the tissue constructs, a fibrinogen solution of 10 mg/mL was prepared in EGM without FBS, and then sterile filtered. HUVECs and fibroblasts at a ratio of 5:1 or HUVECs alone were suspended in the fibrinogen solution. 5% FBS was added to the fibrinogen–cell mixture right before tissue assembly (i.e., mixing the fibrinogen–cell solution with thrombin). In each well of a 24-well plate, 40 μL of a thrombin (Sigma, St. Louis, MO) solution (50 units/mL) was added and mixed with 500 μL of the fibrinogen–cell solution. The plate was left undisturbed for 5 min at room temperature, followed by a 20 min incubation at 37°C to let the fibrinogen polymerize, after which warm EGM-2 was added on top of the fibrin gel. The tissue constructs were maintained at 37°C in 100% humidified air containing 5% CO_2. Medium was changed every 2–3 days. To make tissues that were implanted in immune-compromised mice, 100 μL cell–fibrinogen solution was mixed with 8 μL thrombin in small polydimethylsiloxane (PDMS) chambers (Fig. 1A).

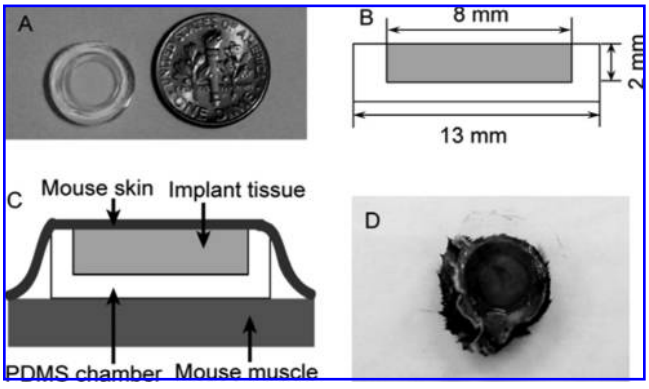

FIG. 1. Fibrin-based tissues were assembled *in vitro* in polydimethylsiloxane (PDMS) circular wells and then implanted with the wells subcutaneously on the dorsal surface of Rag-2 mice with the tissue facing the subdermis of the skin. (**A**) Image of the PDMS circular container. (**B**) Dimensions of the PDMS container. (**C**) Diagram showing tissue constructs that were implanted with the tissue side facing mouse dermis. (**D**) Tissue construct with adjacent mouse skin were harvested 3–14 days postimplant.

Retroviral vector construction and cell transduction

The HUVECs and fibroblasts were transduced with red fluorescent protein (RFP) or green fluorescent protein (GFP) using retroviruses to visualize the endothelial capillaries. The RFP retroviral vector, pBMN-mcherry, was constructed by inserting a 729-bp cassette containing mcherry, which encodes a monomeric RFP (kindly provided by Dr. Roger Tsien, University of California, San Diego, CA), into the pBMN-Z retroviral vector (Orbigen, San Diego, CA). The GFP retroviral vector pBMN-GFP was purchased from Orbigen.

The transduction procedure includes two steps: transfection of the packaging cells (293T; Phoenix Ampho, Orbigen, San Diego, CA), which produces retrovirus containing the fluorescent protein, and infection of the target cells (HUVECs or fibroblasts) with retrovirus. First, the packaging cells were transfected with GFP or RFP vectors using Lipofectamine-2000 (Invitrogen, Carlsbad, CA) according to the manufacturer's instructions. The viral supernatants were collected 48 and 72 h after transfection and filtered through 0.45 μm syringe filter to remove the floating cells. Then, the viral medium together with 5 μg/mL polybrene was added to target cells that were seeded at low density 24 h before the infection. Six hours after the infection, viral medium was replaced with fresh EGM-2 or FGM-2. The infection procedure was performed daily for 4 days. The fraction of cells expressing the fluorescent protein was greater than 80%, and the fluorescence was stable for at least 4 weeks.

Imaging of the in vitro *tissue and optimization of cell seeding density*

Images of the HUVEC capillary networks were taken at days 2, 4, 7, and 14 with an Olympus IX51 microscope equipped with a 100 W high-pressure mercury lamp (Olympus America, Center Valley, PA). Cell seeding densities were optimized to obtain dense, interconnected capillary networks. The ratio of fibroblasts to HUVECs was kept constant at 1:5, while the number of HUVECs was varied from 0.1 million cells per mL to 3 million cells per mL.

The capillaries were quantified (NIH ImageJ) using the following indices: (1) total vessel length (sum of all vessel segments)/mm^2, (2) average length of vessel networks (total vessel length/number of vessel networks), (3) average number of branches per vessel network, and (4) vessel diameter (vessel area/vessel length). Six low-magnification (40×) images of vessel networks for each condition were taken randomly at day 7 to quantify the first three indices. A vessel network was defined as a contiguous length of interconnected capillaries. The number of vessel networks and the number of branches per vessel network were counted manually. Average length of vessel networks was obtained by dividing total vessel length by the number of vessel networks. To quantify the vessel diameter, 10 vessels of each condition were chosen randomly and high-magnification images (100×) of the individual vessels were taken. The projected area and length of the vessels were quantified with ImageJ, and average vessel diameter was calculated by dividing the area by the length.

Implantation of the tissue constructs

Small PDMS containers were made to hold the tissues for the duration of the implantation experiment, and simplify the implantation process. In addition, the chambers limit the

Table 1. Cell Seeding Density and *In Vitro* Culturing Time of Implanted Tissues

Type	*No. of HUVECs*	*No. of fibroblasts*	In vitro *culture time*
I: prevascularised	1×10^6/mL	0.2×10^6/mL	7 days
II: positive control	1×10^6/mL	0.2×10^6/mL	1 day
III: HUVEC only	1×10^6/mL	—	1 day

diffusion of oxygen and nutrients to one side of the tissue, creating a more controlled environment to investigate anastomosis. The dimensions of the container are shown in Figure 1B. Fibrin-based tissues were constructed in the PDMS containers, and the container with the tissue was implanted subcutaneously into immune-deficient Rag-2 mice (Taconic Farms, Oxnard, CA). Animal surgery and animal handling were performed according to NIH guidelines for laboratory animal usage, and our protocol was approved by UCI IACUC. Mice were anesthetized via intraperitoneal injection of 75 mg/kg ketamine and 7 mg/kg xylazine. Two separate pouches underneath the skin were made on the dorsal surface of the animals through blunt dissection between the lower level of the dermis and the fascia over the muscle layer. Each tissue construct was inserted into a pouch with the tissue side facing the dermis (Fig. 1C). The wound was closed with surgical staples. Analgesia was provided via intraperitoneal injection of 10 mg/kg buprenorphin at the completion of the surgery. Animals were sacrificed, and tissues were retrieved at day 3, 5, 7, and 14 after implantation. Mouse skin adjacent to the implanted tissue was also dissected (Fig. 1D).

To compare the *in vivo* performance of prevascularized and nonprevascularized tissues, three types of tissues were implanted: (I) prevascularized tissues in which HUVECs and fibroblasts were seeded 7 days before implantation and thus allowed to develop into well-formed capillary networks; (II) positive control tissues in which both HUVECs and fibroblasts were seeded 24 h before implantation, and thus well-formed capillaries were absent; and (III) tissues containing only HUVECs in which fibroblasts were not incorporated. The cell type, cell density, and *in vitro* culturing time of the three types of tissues are summarized in Table 1. Tissue II is referred to as the positive control because it has been previously demonstrated that HUVEC and fibroblasts distributed throughout a collagen gel formed functional vessels that anastomosed with host vasculature after implantation.[11]

Histology and immunohistochemical staining

Samples were fixed in 10% neutral buffered formalin overnight and embedded in paraffin. Hematoxylin and eosin (H&E), trichrome, and immunohistochemical staining were performed on 4 μm tissue sections. Trichrome staining was carried out using the Modified Gomori's one-step trichrome staining kit (Biocare Medical, Concord, CA). Immunohistochemical staining was performed using the Dako Envision HRP-DAB system (Dako, Carpinteria, CA) according to the manufacturer's instructions after treatment of the sections in Dako Target Retrieval solution at 94°C for 25 min for epitope recovery. The primary antibodies were mouse anti-human CD31 (M0823, diluted at 1:200; Dako) and mouse anti-human Ki67 (M7240, diluted at 1: 75; Dako). Both antibodies were diluted in 0.5 M tris with 1% bovine serum albumin and incubated overnight at 4°C. The secondary antibody used was HRP-conjugated goat anti-mouse immunoglobulins provided by the Dako Envision HRP-DAB system. The bound complex was detected by DAB.

Tissue sections stained with human CD 31 antibody and counter stained with H&E were used to quantify blood perfusion in the implanted tissues. HUVEC-lined vessels with intraluminal erythrocytes were quantified as perfused lumens, while HUVEC-lined lumens without erythrocytes were considered nonperfused lumens. For each condition, a minimum of 10 images from two or three samples implanted in different animals were analyzed.

Statistics

All quantification was performed by three researchers blinded to the conditions. The results are reported as mean ±

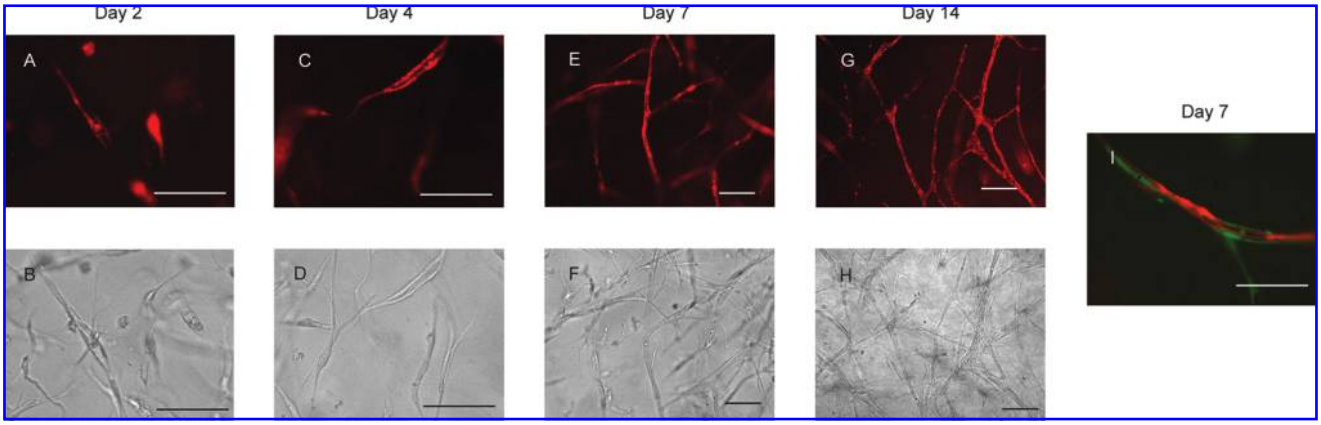

FIG. 2. HUVECs spontaneously form capillary networks within 7 days when cocultured with fibroblasts in a fibrin matrix. HUVECs were transduced with RFP vector (pBMN-mcherry). (**A, B**) HUVECs demonstrated elongated morphology, multicellular structures, and intercellular lumens by day 2. (**C, D**) More mature capillaries with lumens were visible at day 4. (**E, F**) By day 7, three-dimensional capillary networks were formed that remained stable for up to 14 days (**G, H**). (**I**) At day 7, fibroblasts transduced with GFP visibly associated with the HUVEC tube demonstrating pericyte-like behavior *in vitro*. Top panels are fluorescent images, and images in the bottom row are phase contrast. Scale bars: 100 μm. Color images available online at www.liebertonline.com/ten.

standard deviation. Statistical comparisons between conditions were performed using either one-way ANOVA or Student's *t*-test when appropriate. Results are considered statistically significant for $p < 0.05$.

Results

Mature capillary networks form spontaneously in vitro *by 7 days*

Our previous studies demonstrated that HUVECs coated on microbeads can proliferate, migrate, and sprout from the beads to form multicellular capillaries with lumens in the presence of fibroblasts in a fibrin gel.[18,19] However, one drawback of the previous prevascularization model was the presence of undegradable microcarrier beads. In the current model, the beads were removed and the HUVECs and fibroblasts were randomly distributed in the fibrin gel. Two days after embedding in the fibrin gel, HUVECs adopted elongated morphology and formed multicellular structures with intracellular lumens (Fig. 2A, B). By day 4, mature capillaries with lumens were formed (Fig. 2C, D). Anastomosing capillary networks were formed at day 7 (Fig. 2E, F). These capillaries were stable through day 14 (Fig. 2G, H), and no significant difference in any of the endpoints was found between the day 14 capillaries and day 7 capillaries. Fibroblasts demonstrated pericyte-like behavior by closely associating with the endothelial tubes as early as day 7 (Fig. 2I), consistent with capillary maturation.[20] Capillaries did not form in the absence of fibroblasts (data not shown).

In vitro *capillary formation was optimized by varying cell seeding density*

Previous work indicated that a HUVEC:fibroblast ratio of 5:1 is optimal to the growth of capillaries *in vivo*.[11,12] We varied the seeding densities of HUVECs from 0.1 million cells/mL to 3 million cells/mL while keeping the ratio of HUVECs and fibroblasts constant at 5:1 (Fig. 3A–D). Total vessel length, average length of vessel networks, and average number of branches per vessel network were all maximized when the density of HUVECs was 1 million cells per mL (Fig. 3F–H). When the number of HUVECs increased to 3 million/mL, capillary growth decreased with numerous cells demonstrating a spherical morphology consistent with apoptosis. Thus, the optimal cell seeding densities for the *in vivo* studies were determined to be 1 million cells/mL and 0.2 million cells/mL for HUVECs and fibroblasts, respectively.

Prevascularization accelerates the formation of functional anastomoses

To demonstrate functionality of the preformed capillary network *in vivo* and to determine whether prevascularizing an engineered tissue construct can promote blood perfusion, three types of tissues were implanted into Rag-2 immunecompromised mice (Table 1; Fig. 4A–C). H&E stain on the sections of the implanted tissues demonstrated earlier perfusion of the prevascularized tissue compared to the control tissues. Three days postimplantation, multicellular lumens

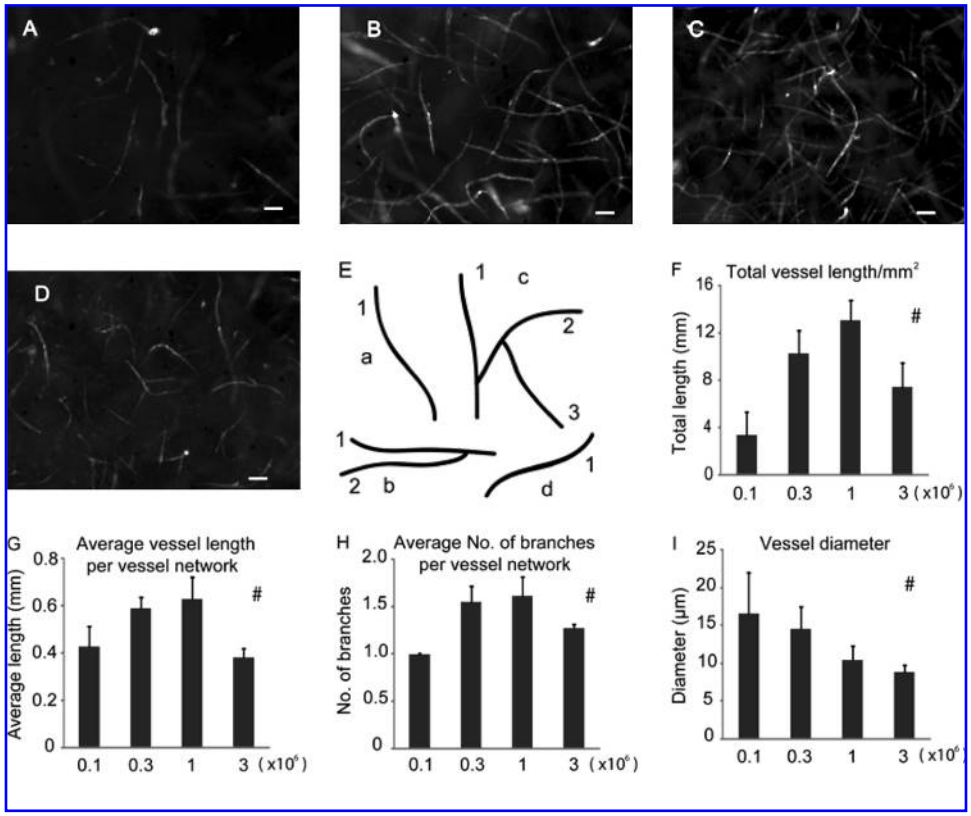

FIG. 3. Optimization of cell seeding density. Optimal seeding density that produced maximal *in vitro* capillary network development by day 7 was determined by varying the total number of HUVECs seeded in each tissue while holding the ratio of fibroblasts to HUVECs constant at 1:5. The densities of HUVECs were 0.1 million/mL (**A**), 0.3 million/mL (**B**), 1 million/mL (**C**), and 3 million/mL (**D**). Scale bars: 100 μm. (**E**) A schematic image showing the technique used to quantify vessel network. Interconnected capillaries were counted as one vessel network. The letters a, b, c, and d indicate four vessel networks, and the numbers indicate branches of each individual network. (**F**) Total vessel length/mm^2. (**G**) Average length of vessel network. (**H**) Average number of branches per vessel network. (**I**) Vessel diameter. #Statistically significant changes with cell seeding densities (one-way ANOVA, $p < 0.05$).

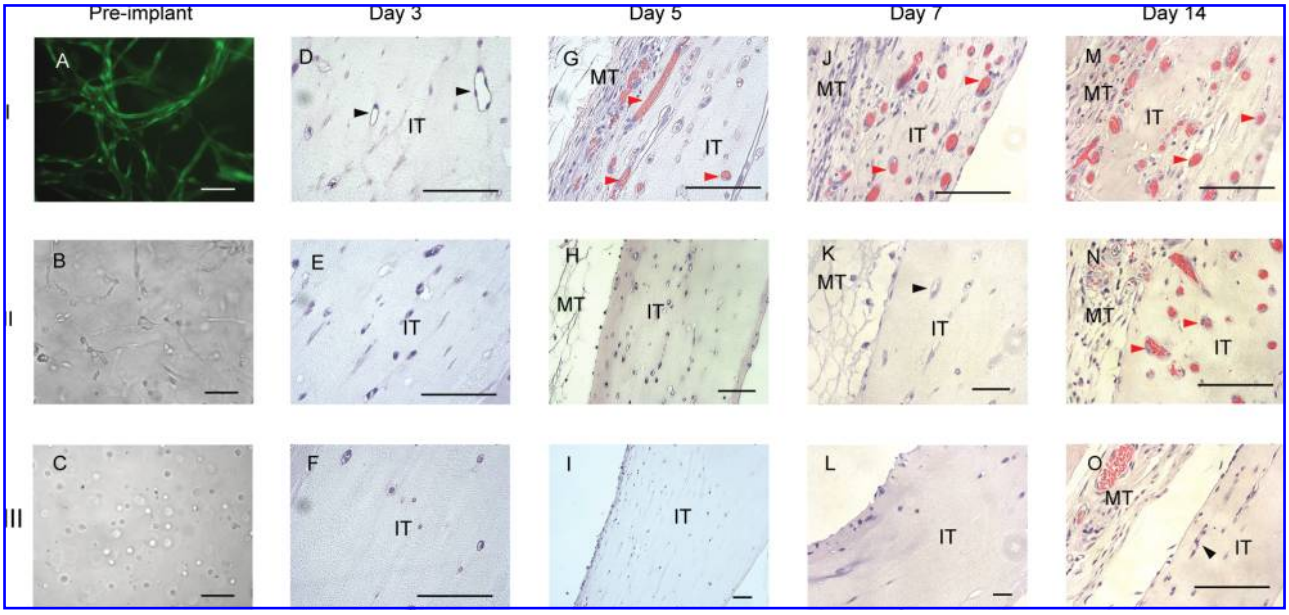

FIG. 4. Prevascularized tissue was perfused by host blood more rapidly than nonprevascularized tissues upon implantation. (**A–C**) Images of prevascularized (tissue I), positive control (tissue II) and HUVEC-only (tissue III) tissues before implant. (**A**) HUVECs were transduced with GFP and demonstrated robust capillary networks in the prevascularized tissue. (**B**) The positive control tissue was comprised of HUVECs and NHLFs coseeded in a fibrin gel 24 h before implant, but no mature capillary structures can be seen by the time of implant. (**D–O**) H&E stain of the tissue sections 3–14 days postimplant. Three days postimplant, vessels with clear lumens were visible in the prevascularized tissue only (black arrowheads, **D**), but no blood flow was observed. Five days postimplant, vessels with red blood cells were evident in the presvascularized tissue (red arrowheads, **G**). By day 7, perfusion of the prevascularized tissue had increased markedly (**J**). Unperfused vessels with lumens in the positive control tissue were now evident (black arrowhead, **K**). By day 14, blood flow was visible in the positive control tissue (**N**). Unperfused vessels with lumens can be seen near the edge of the HUVEC-only tissue (black arrowhead, **O**). MT, mouse tissue; IT, implant tissue. Scale bars: 100 μm. Color images available online at www.liebertonline.com/ten.

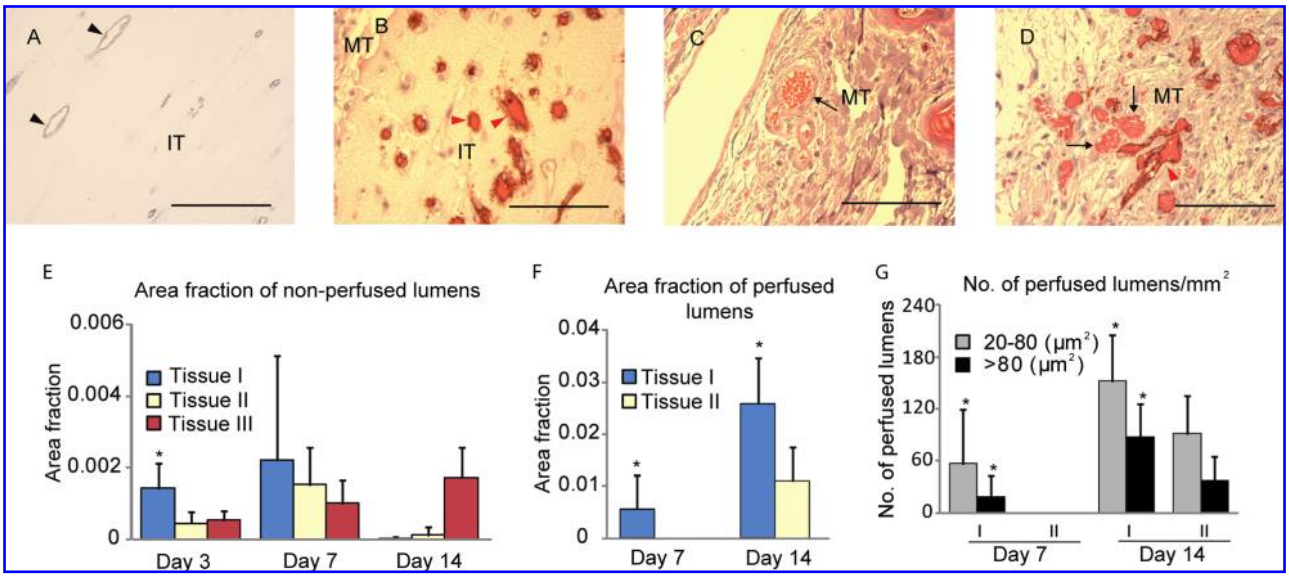

FIG. 5. HUVEC-lined vessels contribute to the perfusion of implanted tissues. (**A, B**) Human CD31 staining of the day 3 (**A**) and day 14 (**B**) prevascularized tissue demonstrated that vessels in the implant were lined by HUVECs. (**C**) Mouse vessels did not cross-react with the human CD31 antibody (black arrow) and were not seen in the implanted tissue. However, near the interface between the mouse tissue and implant tissue, mouse vessels and HUVEC-lined vessels were visible in close proximity, consistent with a site of anastomosis (**D**). Black arrowheads, unperfused vessels lined by HUVECs; red arrowheads, perfused vessels lined by HUVECs; black arrows, mouse vessels; MT, mouse tissue; IT, implanted tissue. Scale bars: 100 μm. (**E–G**) Quantification of the HUVEC-lined vessels. (**E**) The fraction of the cross-sectional image occupied by unperfused lumens. (**F**) The fraction of the area occupied by perfused lumens. (**G**) The number of perfused lumens per unit area. *$p < 0.05$, Student's *t*-test. Color images available online at www.liebertonline.com/ten.

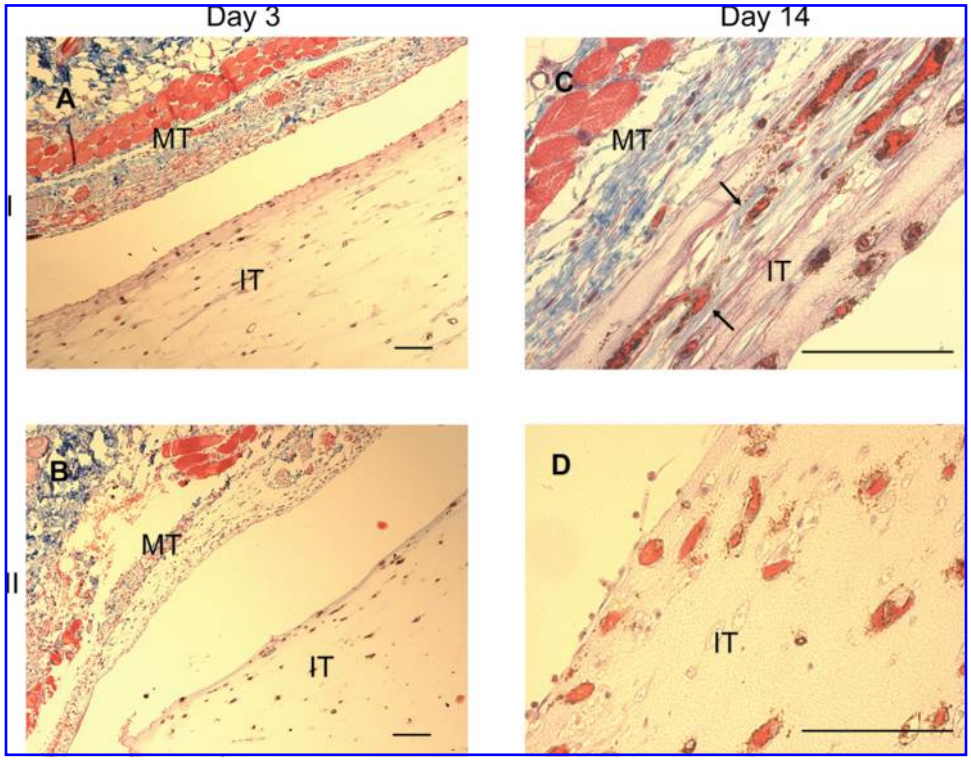

FIG. 6. Collagen deposition in the implanted tissues. Tissue sections were stained with human CD31 antibody followed by trichrome staining to detect collagen deposition in the implanted tissue. At day 3, collagen was not observed in either prevascularized (**A**) or positive control (**B**) tissues. By day 14, HUVEC-lined vessels surrounded by blue collagen fibers were evident in the prevascularized tissue, at the area near mouse tissue (arrows, **C**) but not in the positive control tissue (**D**). MT, mouse tissue; IT, implant tissue. Scale bars: 100 μm. Color images available online at www.liebertonline.com/ten.

absent of blood cells were evident in the prevascularized tissue (tissue I), consistent with more mature vessels. Vessels with red blood cells were evident in the prevascularized tissue by day 5, suggesting anastomosis between days 4–5, and increased markedly at day 7, whereas perfused vessels were not visible in the positive control (tissue II) until day 14, consistent with anastomosis between days 8–14. The tissue containing only HUVECs (tissue III) did not demonstrate any perfusion.

To determine whether these perfused vessels were mouse vessels that infiltrated into the implant, or human vessels perfused via inosculation with the host vasculature, tissue sections were stained with human CD31 antibody. Our results indicate that all the vessels within the implanted tissues, including the nonfunctional vessels with empty lumens (Fig. 5A) and functional vessels containing blood cells (Fig. 5B), were lined by human endothelial cells. Further, human endothelium-lined vessels were in close proximity with mouse vessels near the interface between mouse tissue and implanted tissue, consistent with a site of anastomosis (Fig. 5D).

We next quantified the lumens lined by HUVEC cells in the implanted tissues. Three days postimplant, none of the tissues contained evidence of perfusion, but the prevascularized tissue (I) contained a higher fraction of area occupied by unperfused lumens (Fig. 5E). Seven days postimplant, perfused lumens occupied about 0.5% of the cross-sectional area of the prevascularized tissue (I), but were absent in the positive control tissue (II, Fig. 5F). From day 7 to day 14, the area fraction occupied by perfused lumens increased significantly in the prevascularized (I) and positive control tissues (II), whereas nonperfused lumens were nearly absent in these two types of tissues by day 14 (Fig. 5E). Vessels with empty lumens increased gradually in the tissue containing only HUVECs (III) from day 3 to day 14 with the majority observed close to the mouse skin.

Prevascularization promotes cell proliferation and remodeling

To examine metabolic activity of the tissue constructs *in vivo*, we stained the sections of day 14 prevascularized (I) and positive control (II) tissues with an antibody to Ki67 to examine cell proliferation, and Gomori's Trichrome to examine collagen deposition. There was no evidence of collagen in the day 3 tissue (Fig. 6A); however, collagen fibers were observed in the prevascularized tissue (I), at the area near the mouse tissue, surrounding the HUVEC-lined vessels at day 14 (Fig. 6C), consistent with collagen synthesis *in vivo* after implantation. No evidence of collagen deposition was observed in the positive control tissue (II, Fig. 6B, D). Further, a significantly larger number of proliferating cells (positive Ki67 stain) were present in the prevascularized tissue (I) than the positive control (II, Fig. 7) at day 14.

Discussion

In this study, we constructed three-dimensional HUVEC capillary networks *in vitro*, and demonstrated *in vivo* function of the preformed capillaries in immune-deficient mice. *In vitro*, the HUVECs develop into interconnected capillary networks with lumens within a fibrin gel in the presence of fibroblasts. The fibroblasts are required for capillary formation, and also demonstrate pericyte-like behavior by closely associating with the HUVEC-lined tubes. These well-formed capillary networks anastomosed with the host vasculature within 4–5 days after implantation, whereas a fibrin gel incorporating HUVECs and fibroblasts, but without fully developed capillaries, was perfused by the host blood sometime

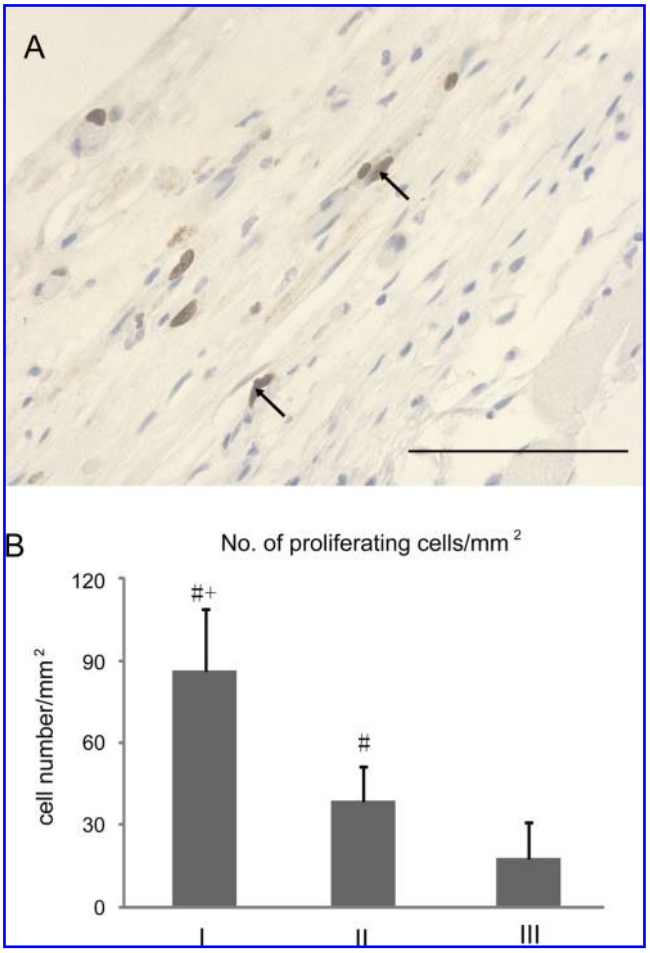

FIG. 7. Cell proliferation in the tissue constructs 14 days postimplant. (**A**) Ki 67 labeling of proliferating cells in the prevascularized tissue (arrows). Scale bar: 100 μm. (**B**) Quantification of proliferating cells. The number of proliferating cells/mm^2 is significantly larger in the prevascularized tissue (tissue I) compared to the positive control (tissue II) and HUVEC-only (tissue III) tissues. $^+$Significantly different from II. $^\#$Significantly different from III. $p < 0.05$, Student's *t*-test. Color images available online at www.liebertonline.com/ten.

between 8 and 14 days after implantation. In addition, tissues with preformed capillaries (prevascularized tissue) were metabolically more active than nonprevascularized tissues, indicated by the presence of collagen deposition and a larger number of proliferating cells.

In vitro *formation of capillary networks*

Our previous work demonstrated that HUVECs coated on microcarrier beads embedded in a fibrin gel with a monolayer of fibroblasts 2 mm away sprout capillaries with lumens, mimicking the process of angiogenesis.[18] In the present work, the spontaneous *in vitro* formation of capillaries from randomly distributed endothelial cells and fibroblasts mimics the process of vasculogenesis, or the *de novo* formation of vessels from endothelial cells. It has been demonstrated that fibroblasts promote angiogenesis *in vitro* and *in vivo*, in part through the secretion of soluble mediators that diffuse through the matrix to the endothelial cells.[20–23] However, the precise mechanism (or mediators secreted by the fibroblast) remains unknown. This study, along with our previous results,[20] supports the concept that fibroblasts can also support endothelial tube formation through direct contact with endothelial cells.

We chose the ratio of HUVECs and fibroblasts to be 5:1 based on previous reports.[11,12] This ratio was kept constant during the optimization of cell seeding density. Hence, while we sought an optimal density of cells, we may be able to achieve even more rapid perfusion in the implanted tissue by examining the ratio of fibroblasts to endothelial cells. An interconnected network of capillaries is a potentially desirable feature to accelerate perfusion, as one might imagine that only a single anastomosis with the host is required to perfuse the entire network. In addition, a more branched network may also be desirable to minimize the distance between an interstitial cell and a capillary. Hence, our *in vitro* endpoints included not only the total vessel network length but also the average length of continuous vessel networks and the number of branches per network. All three indices peaked at 1 million endothelial cells per mL.

In vivo *function of the preformed capillary networks*

We hypothesized that prevascularizing an engineered tissue construct with well-formed vascular networks would accelerate the formation of functional vasculature upon implantation, and eventually promote survival of the implanted tissue. Our results showed that prevascularized tissue was perfused with mouse blood between 4–5 days, significantly earlier than nonprevascularized tissues (between 8 and 14 days, Fig. 4). The evidence that perfused lumens in the implanted tissues were lined by HUVECs (Fig. 5B), combined with close proximity of mouse vessels with HUVEC-lined vessels (Fig. 5D), suggests anastomosis of HUVEC-lined vessels with mouse vessels, rather than incorporation of HUVECs within an infiltrating mouse vessel.

In our experiments, the preformed capillaries began to anastomose with the host vasculature 4–5 days postimplant. This time frame may not be adequate for oxygen-sensitive tissues such as hepatocytes or cardiac myocytes. However, we did not attempt to minimize this time frame in the current study, only to demonstrate superior performance of the preformed capillaries. Previous studies demonstrated that unprevascularized implantable gel constructs (similar to our control tissues) anastomosed with host vasculature at day 7, which is faster than our control tissues.[11,26] Manipulating variables such as the ratio of endothelial cells to stromal cells, the fibrin concentration,[19] the time of *in vitro* culture, or the addition of exogenous growth factors (e.g., VEGF or bFGF) may reduce the time needed for functional anastomoses and account for differences between our results and those from previous reports. Nonetheless, our results suggest that the time frame for vascularization typically achieved *in vivo* during wound healing ($\sim$ 2 days) is a viable target.

Tremblay *et al.*[17] constructed a prevascularized skin equivalent by coseeding keratinocytes, fibroblasts, and HUVECs on a collagen sponge and transplanted the construct to nude mice after 31 days of *in vitro* culture. In their study, HUVECs formed capillary-like structures *in vitro*, and host blood was observed within the HUVEC-lined vessels 4 days after implantation, a similar result to our study,

although our construct required only 7 days of *in vitro* culture. In addition, the perfused vessel density in the tissue constructs was relatively low (<10 vessels/mm^2 compared to ~100 vessels/mm^2 in our current study), which may reflect the differences in the design of the prevascularized tissue (e.g., HUVEC-to-fibroblast ratio) that has not been optimized, and may be tissue specific.

Finally, in addition to earlier perfusion, we also observed collagen deposition, and enhanced cell proliferation in the prevascularized tissue. Both of these processes require oxygen and energy, suggesting that the prevascularized tissue is not only perfused, but also receiving adequate oxygen to facilitate metabolic activity.

Strategies for vascularizing engineered tissues

An implanted tissue relies on diffusion to survive before a circulation system is established between the host and the implant. This restriction is a critical obstacle in the design of large three-dimensional engineered tissue. In addition to our proposed method of prevascularizing with a well-formed capillary network, competing technologies include the controlled release of proangiogenic growth factors (e.g., vascular endothelial growth factor or platelet-derived growth factor) from the tissue implant[24,25] and seeding the tissue with endothelial and/or stromal cells (similar to our positive control). It has been demonstrated that human ECs transplanted into immune-compromised mouse on biodegradable polymers or collagen gels formed functional human vessels that anastomosed with mouse vasculature.[7,8] Transduction of the ECs with human telomerase reverse transcriptase or anti-apoptotic *Bcl-2* gene can promote EC survival and vascularization of implanted tissue.[9,10] Coseeding of endothelial cells and fibroblasts resulted in long-lasting vessels that were functional *in vivo* for over a year.[11] However, the time for ECs to develop into functional vessels was relatively long (1–2 weeks).

Application of the tissue model

We used HUVECs in this study because they are easily extracted from an available supply of discarded umbilical cords, and can be expanded to relatively large numbers. While HUVECs do not solve the problem of immune compatibility for a cellularized tissue implant, endothelial progenitor cells from blood[26,27] and other sources (e.g., fat tissue)[28–30] have also demonstrated angiogenic potential *in vivo* and *in vitro*. Thus, these cells may be used to create well-formed capillary networks for implantable tissues in immune competent animal models, and ultimately humans in the future.

The current model of vasculogenesis provides a platform to study the relationship between *in vitro* morphology and *in vivo* function of engineered capillary networks. For example, the prevascularized tissue (I) and the positive control (II) had the same starting components (i.e., fibrin concentration and number and type of cells). The only difference was that the prevascularized tissue had been cultured *in vitro* for 7 days in an oxygen- and nutrient-rich environment before implantation allowing the HUVECs to assemble into a well-formed capillary network. Our results suggest that this difference in morphology accelerates vessel perfusion and tissue remodeling. While the total time from tissue formation (*in vitro* time plus *in vivo* time) to blood perfusion may be similar between the two tissues (11–12 days for prevascularized tissue, and 9–15 days for the positive control), the acceleration of blood perfusion *in vivo* clearly suggests an advantage of allowing the capillaries to develop *in vitro*. Numerous additional morphologies such as branching and continuity of the network are potential variables for optimization in future studies, and may be tailored to meet the vascular needs of specific tissues.

Conclusion

We have demonstrated that prevascularizing a tissue with a well-formed capillary network accelerates the formation of functional anastomoses with the host vasculature, leading to earlier perfusion and metabolic activity in the implanted tissue. The tissue design has the flexibility to utilize alternate sources of endothelial and stromal cells. Future work must attempt to minimize the time necessary to achieve perfusion by manipulating such variables as the ratio of endothelial and stromal cells, as well as demonstrate the functional significance of achieving a thicker viable tissue.

Acknowledgments

We appreciate the technical expertise of Mr. Joseph Harris. We acknowledge Dr. Roger Tsien, University of California, San Diego, for the kind gift of pCDNA3-mcherry vector. We also thank Mr. Bhupinder Shergill, Mr. Chong Wang, and Mr. Jason Luo for their assistance in quantifying the *in vitro* and *in vivo* vascular networks. This work was supported in part by grants from the National Institutes of Health (R01 HL067954 [S.C.G.], R01 HL085339 [A.J.P.], and R01 HL086959 [C.C.W.H.]), as well as the Whitaker Foundation, and the Multi-investigator research grants from the Committee on Research and Library Resources from the University of California, Irvine.

Disclosure Statement

No competing financial interests exist.

References

1. Vacanti, J.P., and Langer, R. Tissue engineering: the design and fabrication of living replacement devices for surgical reconstruction and transplantation. Lancet **354 Suppl 1,** SI32, 1999.
2. Wisser, D., and Steffes, J. Skin replacement with a collagen based dermal substitute, autologous keratinocytes and fibroblasts in burn trauma. Burns **29,** 375, 2003.
3. Rodriguez, A., Cao, Y.L., Ibarra, C., Pap, S., Vacanti, M., Eavey, R.D., and Vacanti, C.A. Characteristics of cartilage engineered from human pediatric auricular cartilage. Plastic Reconstr Surg **103,** 1111, 1999.
4. Nillesen, S.T., Geutjes, P.J., Wismans, R., Schalkwijk, J., Daamen, W.F., and van Kuppevelt, T.H. Increased angiogenesis in acellular scaffolds by combined release of FGF2 and VEGF. J Control Release **116,** e88, 2006.
5. Chen, R.R., Silva, E.A., Yuen, W.W., and Mooney, D.J. Spatio-temporal VEGF and PDGF delivery patterns blood vessel formation and maturation. Pharm Res **24,** 258, 2007.
6. Sahota, P.S., Burn, J.L., Brown, N.J., and MacNeil, S. Approaches to improve angiogenesis in tissue-engineered skin. Wound Repair Regen **12,** 635, 2004.

7. Nor, J.E., Peters, M.C., Christensen, J.B., Sutorik, M.M., Linn, S., Khan, M.K., Addison, C.L., Mooney, D.J., and Polverini, P.J. Engineering and characterization of functional human microvessels in immunodeficient mice. Lab Invest **81,** 453, 2001.
8. Twardowski, T., Fertala, A., Orgel, J.P., and San Antonio, J.D. Type I collagen and collagen mimetics as angiogenesis promoting superpolymers. Curr Pharm Des **13,** 3608, 2007.
9. Yang, J., Nagavarapu, U., Relloma, K., Sjaastad, M.D., Moss, W.C., Passaniti, A., and Herron, G.S. Telomerized human microvasculature is functional *in vivo*. Nat Biotechnol **19,** 219, 2001.
10. Schechner, J.S., Nath, A.K., Zheng, L., Kluger, M.S., Hughes, C.C., Sierra-Honigmann, M.R., Lorber, M.I., Tellides, G., Kashgarian, M., Bothwell, A.L., and Pober, J.S. *In vivo* formation of complex microvessels lined by human endothelial cells in an immunodeficient mouse. PNAS **97,** 9191, 2000.
11. Koike, N., Fukumura, D., Gralla, O., Au, P., Schechner, J.S., and Jain, R.K. Tissue engineering: creation of long-lasting blood vessels. Nature **428,** 138, 2004.
12. Levenberg, S., Rouwkema, J., Macdonald, M., Garfein, E.S., Kohane, D.S., Darland, D.C., Marini, R., van Blitterswijk, C.A., Mulligan, R.C., D'Amore, P.A., and Langer, R. Engineering vascularized skeletal muscle tissue. Nat Biotechnol **23,** 879, 2005.
13. Caspi, O., Lesman, A., Basevitch, Y., Gepstein, A., Arbel, G., Habib, I.H., Gepstein, L., and Levenberg, S. Tissue engineering of vascularized cardiac muscle from human embryonic stem cells. Circ Res **100,** 263, 2007.
14. Shin, M., Matsuda, K., Ishii, O., Terai, H., Kaazempur-Mofrad, M., Borenstein, J., Detmar, M., and Vacanti, J.P. Endothelialized networks with a vascular geometry in microfabricated poly(dimethyl siloxane). Biomed Microdev **6,** 269, 2004.
15. Peters, M.C., Polverini, P.J., and Mooney, D.J. Engineering vascular networks in porous polymer matrices. J Biomed Mater Res **60,** 668, 2002.
16. Black, A.F., Berthod, F., L'Heureux, N., Germain, L., and Auger, F.A. *In vitro* reconstruction of a human capillary-like network in a tissue-engineered skin equivalent. FASEB J **12,** 1331, 1998.
17. Tremblay, P.L., Hudon, V., Berthod, F., Germain, L., and Auger, F.A. Inosculation of tissue-engineered capillaries with the host's vasculature in a reconstructed skin transplanted on mice. Am J Transplant **5,** 1002, 2005.
18. Griffith, C.K., Miller, C., Sainson, R.C., Calvert, J.W., Jeon, N.L., Hughes, C.C., and George, S.C. Diffusion limits of an *in vitro* thick prevascularized tissue. Tissue Eng **11,** 257, 2005.
19. Ghajar, C.M., Blevins, K.S., Hughes, C.C., George, S.C., and Putnam, A.J. Mesenchymal stem cells enhance angiogenesis in mechanically viable prevascularized tissues via early matrix metalloproteinase upregulation. Tissue Eng **12,** 2875, 2006.
20. Ghajar, C.M., Chen, X., Harris, J.W., Suresh, V., Hughes, C.C., Jeon, N.L., Putnam, A.J., and George, S.C. The effect of matrix density on the regulation of 3-D capillary morphogenesis. Biophys J **94,** 1930, 2008.
21. Hughes, C.C. Endothelial-stromal interactions in angiogenesis. Curr Opin Hematol **15,** 204, 2008.
22. Velazquez, O.C., Snyder, R., Liu, Z.J., Fairman, R.M., and Herlyn, M. Fibroblast-dependent differentiation of human microvascular endothelial cells into capillary-like 3-dimensional networks. FASEB J **16,** 1316, 2002.
23. Liu, H., Chen, B., and Lilly, B. Fibroblasts potentiate blood vessel formation partially through secreted factor TIMP-1. Angiogenesis **11,** 223, 2008.
24. Richardson, T.P., Peters, M.C., Ennett, A.B., and Mooney, D.J. Polymeric system for dual growth factor delivery. Nature Biotech **19,** 1029, 2001.
25. Wong, C., Inman, E., Spaethe, R., and Helgerson, S. Fibrin-based biomaterials to deliver human growth factors. Thromb Hemost **89,** 573, 2003.
26. Melero-Martin, J.M., Khan, Z.A., Picard, A., Wu, X., Paruchuri, S., and Bischoff, J. *In vivo* vasculogenic potential of human blood-derived endothelial progenitor cells. Blood **109,** 4761, 2007.
27. Kalka, C., Masuda, H., Takahashi, T., Kalka-Moll, W.M., Silver, M., Kearney, M., Li, T., Isner, J.M., and Asahara, T. Transplantation of *ex vivo* expanded endothelial progenitor cells for therapeutic neovascularization. PNAS **97,** 3422, 2000.
28. Planat-Benard, V., Silvestre, J.S., Cousin, B., Andre, M., Nibbelink, M., Tamarat, R., Clergue, M., Manneville, C., Saillan-Barreau, C., Duriez, M., Tedgui, A., Levy, B., Penicaud, L., and Casteilla, L. Plasticity of human adipose lineage cells toward endothelial cells: physiological and therapeutic perspectives. Circulation **109,** 656, 2004.
29. Levenberg, S. Engineering blood vessels from stem cells: recent advances and applications. Curr Opin Biotechnol **16,** 516, 2005.
30. Urbich, C., and Dimmeler, S. Endothelial progenitor cells functional characterization. Trends Cardiovasc Med **14,** 318, 2004.

Address reprint requests to:
Steven C. George, M.D., Ph.D.
Department of Biomedical Engineering
Natural Science II, Room 3125
University of California Irvine
Irvine, CA 92697-2715

E-mail: scgeorge@uci.edu

Received: June 1, 2008
Accepted: August 26, 2008
Online Publication Date: October 24, 2008